

## **DISTRIBUTION OF PLASTIC STRAINS IN FIR-WOOD AT STATIC BENDING**

SLAVKO GOVORČIN, TOMISLAV SINKOVIĆ, RADOVAN DESPOT  
FORESTRY FACULTY OF ZAGREB UNIVERSITY, ZAGREB, CROATIA

### **ABSTRACT**

The distribution of strains at static bending within the plastic range is interesting, since the model is similar to the real distribution. Both longitudinal and tangential strains caused by static bending with single-load application in the centre of a 20x20x300 mm sample were determined by analysing the video-records of the static bending. According to the research results, this method is suitable, if some improvements are made. The obtained distribution in tangential direction shows the presence of tensile strains during static bending. The distribution of strains in longitudinal direction shows similarity to the so far used models, which, however, has not been entirely confirmed statistically.

**KEY WORDS:** static bending, plastic strains, fir-wood (*Abies alba Mill.*)

### **INTRODUCTION**

Strains in wood at static bending can be divided into two groups, elastic and plastic. Accepting the linear relation between stress and strain has solved the problem with wood strains in the elastic range. Stress distribution was thus defined according to the beam height and the position of the neutral line. Wood strains in the plastic range are not distributed in a linear manner and the position of the neutral line changes with load increase.

The to date research on determining a model of stress distribution within the plastic range, as well as the movements of the neutral line are based on graphic and mathematical models. The first solutions to the problem (Baumann 1922 compared to Kollmann, Côte 1968) were graphic. The disadvantages of the solutions encouraged other researchers (Roš 1936, Thunell 1939 and 1940 compared to Kollmann, Côte 1968) to apply more realistic approximations using a trapezoid form of distribution. The parabola in the compression range and the straight line in the tensile range were taken as a model closest to reality. According to available literature, (Karlsen 1961 compared to Zakić 1976), Zakić (1976) and Baas (1982) also used a parabola in the compression range and a straight line in the tensile range of the beam, as a strain distribution model.

The research aim is to determine longitudinal and tangential strains in the point of proportionality, two moments just before breaking and at the very moment of breaking. For this purpose, a new method of determining strains was used. Based on strain measuring

by means of a tensiometer, this method enables simultaneous strain determination both in longitudinal and tangential directions. This research will also evaluate the new method.

## MATERIAL AND METHODS

Firwood (*Abies Alba Mill.*) samples, crosscut, in dimensions 20x 20x 300 mm were used for the research. The load was applied in the middle, between the supports. During the research, the moisture content was about 30%. In spite of the effects of the slipping strain, and the high level of water content, the single-load system was chosen because of increased strains and their simpler measurement. A net of horizontal and vertical lines, 2 mm apart, was applied to the tangential cross-section of the sample using the silk-screen process. The whole process of specimen static bending was recorded with an S-VHF resolution video camera (Fig. 1).

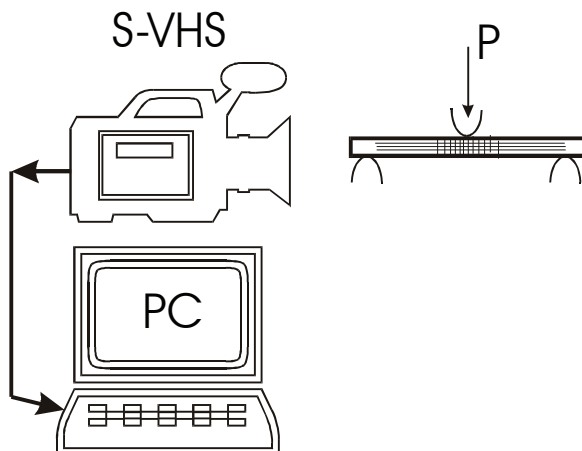


Fig. 1: The sample with silk-screen-printed lines. S-VHF camera for recording the bending process

Five photographs were chosen relating to the following moments: (1) before bending; (2) when the load was approximately at the proportionality points (PI); (3) when the effecting force was by 8% smaller than the breaking force ( $P_{\max-8\%}$ ); when the effecting force was by 4% smaller than the breaking force ( $P_{\max-4\%}$ ), and when the sample broke, i.e. at maximum force ( $P_{\max}$ ).

The photos were transformed into a bigger resolution and enlarged three times. Using the Scion Image Release Beta 3b computer programme, the co-ordinates of horizontal and vertical line cross-sections were read off. The vertical line was situated precisely below the point of force (the line between the central part of the tool curvature, perpendicular upon the sample in tangential direction), and upon the horizontal lines that were the 2 mm-lengths from the central line, both right and left. The changes upon ten lines in tangential direction, and eleven lines in longitudinal direction were measured on the sample. In tangential direction, line 1 was the nearest, while line 10 was the most distant from the place of force exertion. In longitudinal

direction, line 1 is situated upon the upper rim of the sample, the closest position to the force exertion, while line 11 on the lower sample rim is the most distant from where the force is exerted. The distribution of the measuring spots is shown in Fig. 2.

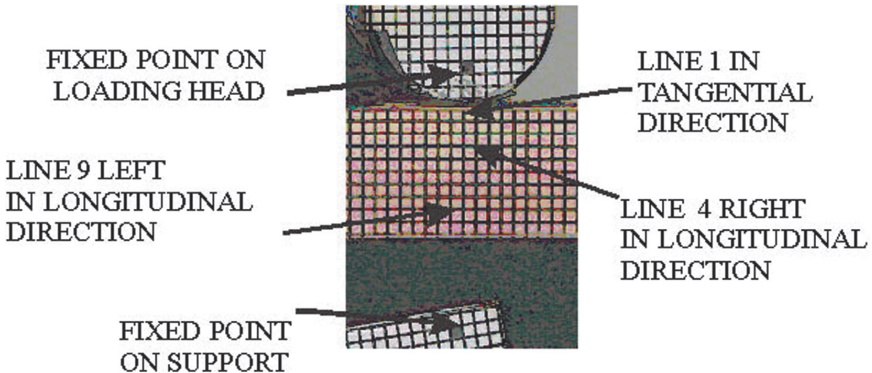


Fig. 2: Distribution of measurement points on the sample

The resolution of the video camera and the graphic card enabled accurate measurement of the relative extension by 0.02 mm. The research was done at the time when S-VHS resolution was the highest available, compared to today's digital camera resolutions of 1000x1000 pixels. Relative extensions of the measured lines were calculated by formula (1), where  $l_1$  is the length at certain test moments, while  $l$  is the initial length.

$$\epsilon = \frac{l_1 - l}{l} = \frac{\Delta l}{l} \quad (1)$$

Equation (1) was set in order to distinguish compression strains (-) from tensile strains (+). The mean value and the reliability interval of 95% were calculated by using the measurement data of the relative extensions. The forces in the points of proportionality and maximum forces were determined from the deflection and force diagrams. The deflections in the proportionality points and breaking points were determined on the basis of the difference between the distance of the reference point upon the bending tool and the supports (Fig. 2). Deflections both in the proportionality point and at maximum force were checked on the strain/force diagram obtained on test machine.

## RESULTS AND DISCUSSION

Seventeen fir samples were used for the research on static bending. Relevant statistical indices of their initial dimensions, measurement results and calculated properties are shown in Tab. 1.

Tab. 1: Relevant statistical indicators of initial dimensions, measurement results and calculated results for all samples

	n	h [mm]	$P_{\max}$ [N]	$P_{pl}$ [N]	$f_{\max}$ [mm]	$f_{pl}$ [mm]	$\rho_0$ [g/cm <sup>3</sup> ]	$\sigma_{bw}$ [MPa]	$\sigma_{b12}$ [MPa]	W [%]
MV	20.2	2.12	1040	571	12.29	3.06	0.4406	46.3	84.7	29.3
MIN	8	2.06	815	390	9	2	0.3661	36.1	62.4	25.9
MAX	42	2.18	1400	980	18	4.7	0.5246	60.9	118.3	34.4
STD	10.34	0.037	188.21	121.70	2.157	0.729	0.04361	7.22	14.76	2.484

n – number of annual rings in the sample, h – sample height in tangential direction,  $P_{\max}$  – breaking load,  $P_{pl}$  – load at point of proportionality,  $f_{\max}$  – deflection at breaking load,  $f_{pl}$  – deflection at point of proportionality,  $\rho_0$  – density in absolutely dry condition,  $\sigma_{bw}$  – statistical bending strength,  $\sigma_{b12}$  – statistical bending strength at 12% moisture content, W – moisture content, MV – mean value, MIN – minimum value, MAX – maximum value, STD – standard deviation.

There were attempts to interpret the obtained results according to the model of the second-degree parabola in compression rang and the straight line in tensile rang along the beam height. The calculation of the parabola and line parameters showed that, unfortunately, the correlation coefficient ( $R^2$ ) is too small, i.e. up to 0.25. The calculation of mean values and the 95%-reliability intervals of the mean values per lines are considered more appropriate. The result interpretation by mean values is in this case more reliable. The differences in the result interpretation are shown in Fig. 3.

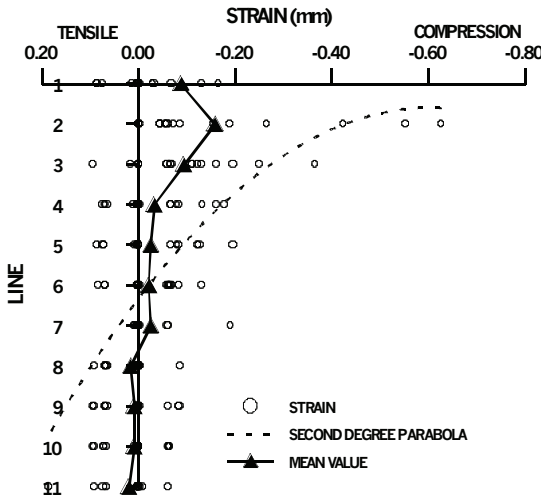


Fig. 3: Distribution of measurement results, regression curve and the mean values of strains at longitudinal break along the lines to the right of load exertion

Relevant statistical indicators of strains per lines and loads in longitudinal direction for seventeen fir samples are shown in Tab. 2.

Tab. 2: Relevant statistical indicators of strains per lines and loads in longitudinal direction for seventeen fir samples

LINE	POSITION	LOAD							
		Ppl		Pmax-8%		Pmax-4%		Pmax	
		LEFT	RIGHT	LEFT	RIGHT	LEFT	RIGHT	LEFT	RIGHT
1	MV	-0.01	-0.02	0.00	0.00	-0.01	-0.01	-0.08	-0.09
	STD	0.07	0.07	0.06	0.06	0.07	0.07	0.12	0.17
2	MV	0.00	-0.01	-0.05	-0.07	-0.03	-0.08	-0.14	-0.16
	STD	0.07	0.07	0.05	0.15	0.24	0.19	0.13	0.20
3	MV	-0.01	-0.01	-0.03	-0.04	-0.05	-0.05	-0.09	-0.09
	STD	0.04	0.05	0.06	0.11	0.07	0.13	0.14	0.11
4	MV	-0.01	0.00	-0.03	0.01	-0.04	-0.01	-0.08	-0.03
	STD	0.04	0.05	0.05	0.07	0.05	0.07	0.09	0.08
5	MV	0.00	0.00	0.00	0.00	0.00	-0.01	-0.04	-0.03
	STD	0.05	0.05	0.05	0.05	0.05	0.05	0.10	0.08
6	MV	-0.01	0.00	-0.01	0.00	-0.01	0.00	-0.04	-0.02
	STD	0.04	0.05	0.06	0.06	0.05	0.06	0.06	0.06
7	MV	0.00	-0.01	0.00	0.01	0.00	0.01	0.00	-0.02
	STD	0.05	0.05	0.05	0.04	0.04	0.04	0.04	0.05
8	MV	-0.01	0.02	0.00	0.01	0.00	0.02	-0.01	0.02
	STD	0.05	0.05	0.06	0.06	0.06	0.07	0.05	0.04
9	MV	0.01	0.01	0.02	0.00	0.02	0.01	0.02	0.01
	STD	0.06	0.04	0.05	0.06	0.06	0.06	0.04	0.05
10	MV	0.00	0.00	0.02	0.01	0.00	0.03	0.02	0.01
	STD	0.05	0.05	0.05	0.06	0.05	0.06	0.07	0.05
11	MV	0.01	0.01	0.01	0.01	0.01	0.02	0.02	0.02
	STD	0.06	0.05	0.04	0.06	0.06	0.05	0.05	0.06

$P_{pl}$  – load at proportional limit;  $P_{max-8\%}$  – load was by 8% weaker than breaking load;  $P_{max-4\%}$  – load was by 4% weaker than breaking load;  $P_{max}$  – breaking load; MV – mean value and STD – standard deviation.

Fig. 4 and 5 show mean values of strains in longitudinal direction, to the left and right respectively, of the load exertion line.

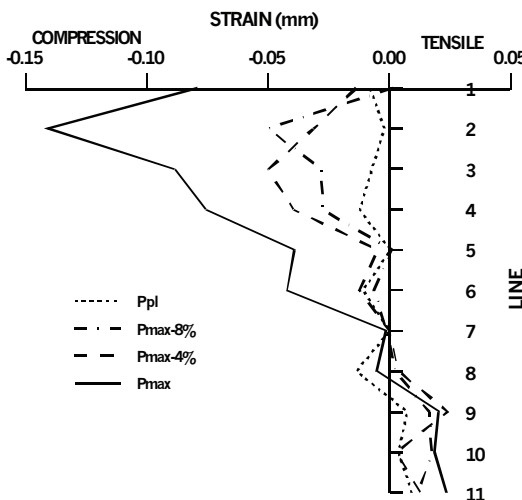


Fig. 4: Distribution of mean values of strains in longitudinal direction on the lines left of load exertion

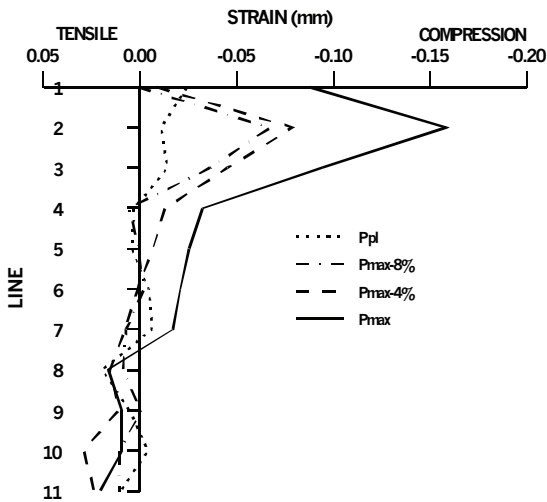


Fig. 5: Mean values of strains in longitudinal direction on the lines to the right of load exertion

The intersections of the lines connecting the mean values of the relative extensions and the zero-lines present the position/or approximate position of the neutral line upon the longitudinal direction. The mean values of the strains in Tab. 2 and their illustration in Fig. 4 and 5 show that, with increased force between the proportionality point and the breaking point – in the positions where compression strains turn into tensile strains – the neutral line moves from the middle height of the sample toward its lower part.

Relevant statistical indicators of strains per lines and loads in tangential direction for seventeen fir samples are shown in Tab. 3.

Tab. 3: Relevant statistical indicators of strains per lines and loads in tangential direction for seventeen fir samples

LINE		LOAD			
		P <sub>pl</sub>	P <sub>max-8%</sub>	P <sub>max-4%</sub>	P <sub>max</sub>
1	MV	-0.02	-0.17	-0.18	-0.17
	STD	0.09	0.14	0.14	0.16
2	MV	0.00	-0.06	-0.10	-0.17
	STD	0.06	0.09	0.10	0.18
3	MV	-0.02	-0.04	-0.05	-0.08
	STD	0.07	0.06	0.05	0.07
4	MV	0.01	-0.01	-0.01	-0.03
	STD	0.04	0.05	0.04	0.07
5	MV	0.00	-0.03	-0.04	-0.05
	STD	0.05	0.04	0.04	0.09
6	MV	-0.01	-0.03	-0.03	-0.06
	STD	0.06	0.04	0.05	0.06
7	MV	0.00	-0.02	-0.03	-0.06
	STD	0.05	0.05	0.05	0.08
8	MV	0.03	0.01	-0.02	-0.03
	STD	0.07	0.07	0.06	0.09
9	MV	-0.01	-0.01	0.00	-0.03
	STD	0.06	0.07	0.06	0.07
10	MV	-0.02	-0.03	-0.01	-0.03
	STD	0.05	0.05	0.07	0.07

P<sub>pl</sub> – load at proportional limit; P<sub>max-8%</sub> – load was by 8% weaker than breaking load; P<sub>max-4%</sub> – load was by 4% weaker than breaking load; P<sub>max</sub> – breaking load; MV – mean value and STD – standard deviation.

Mean strain values in tangential direction are shown in Fig. 6.

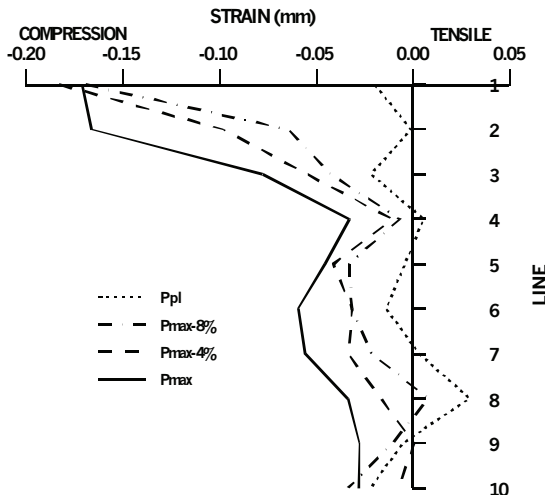


Fig. 6: Mean values of strains in tangential direction

The intersections of the lines connecting the mean values of the relative extensions and the zero-lines present the position/or approximate position of the neutral line upon the tangential direction. The mean values of the strains in tangential directions (Tab. 3) and their illustration in Fig. 6 show that tensile strains appear with the force in tangential directions at the point of proportionality. They also appear with the force that is by 8% smaller than the breaking force. These tensile strains appear along the lines that are below the middle height of the sample. The appearance of the described tensile strains does not conform to the present models. Fig. 4, 5 and 6 clearly show that the increase of the force from the point of proportionality to the breaking force moves the neutral line from the centre of the sample to its lower part.

## CONCLUSIONS

The longitudinal distribution of strains is not equal on the left and right sides (2 mm) from the central line of force exertion.

The tangential distribution of strains indicates that they are not only compression strains, except for the breaking moment.

These measurements did not reveal the distribution of parabola-shaped strains in the compression range and the lines in the tensile range, since the correlation coefficients are too small.

The distribution of strains in longitudinal directions on figures 3 and 4 shows that the strains on the lines that are the nearest to the place of force exertion are parabola-shaped. By moving downward from the place of compression force, the strains turn tensile, while their distribution resembles a line.

The intersection of lines connecting the mean values of strains to the zero line on the graphs present the position of the neutral axis at four load moments. They show that the neutral axis shifts downward from the height centre of the sample, increasing the load from the proportionality point to the breaking point.

The employed method of determining strains has proved appropriate for this kind of research. Since the S-VHS camera was acquired in 1996, its resolution was then the highest possible. In the following years, the improvements of the more available software enabled the given measurement accuracy. With considerably higher resolutions of today's software, the increased measurement accuracy can compete with the precision of the tensiometer.

## REFERENCES

1. Baas, P., 1982: New Perspectives in Wood Anatomy, Published on the occasion of the 50<sup>th</sup> Anniversary of the International Association of Wood Anatomists, Martinus Nijhoff/Dr. W. Junk publishers, the Hague/Boston/London, 151-222 pp.
2. Kollmann, F. F. P.; Côte, W. A., 1968: Principles of Wood Science and Technology. Vol. 1. Solid Wood. Springer Verlag, Berlin-Heidelberg- New York, 592 pp.
3. Zakić, B. D., 1976: Stress Distribution within the Plastic Range in Wood Beam Subjected to Pure Bending. Holzforschung und Holzverwertung, 28(5): 114-120

Doc. Dr. SC. SLAVKO GOVORČIN  
FORESTRY FACULTY OF ZAGREB UNIVERSITY  
DEPARTMENT OF WOOD SCIENCE  
SVETOŠIMURSKA 25  
10 002 ZAGREB  
CROATIA  
TEL: + 385 1 235 2512  
E-mail: slavko.govorcin@zd.htnet.hr

DR. SC. TOMISLAV SINKOVIĆ  
FORESTRY FACULTY OF ZAGREB UNIVERSITY  
DEPARTMENT OF WOOD SCIENCE  
SVETOŠIMURSKA 25  
10 002 ZAGREB  
CROATIA

Doc. Dr. SC. RADOVAN DESPOT,  
FORESTRY FACULTY OF ZAGREB UNIVERSITY  
DEPARTMENT OF WOOD SCIENCE  
SVETOŠIMURSKA 25  
10 002 ZAGREB  
CROATIA

